Inorganic Chemistry

COMMUNICATION

pubs.acs.org/IC

Toward Functional Ni-SOD Biomimetics: Achieving a Structural/Electronic Correlation with Redox Dynamics

Eric M. Gale,[†] Andrew C. Simmonett,[†] Joshua Telser,[‡] Henry F. Schaefer, III,[†] and Todd C. Harrop*[,†]

[†]Department of Chemistry and Center for Computational Chemistry, The University of Georgia, 1001 Cedar Street, Athens, Georgia 30602, United States

[‡]Department of Biological, Chemical and Physical Sciences, Roosevelt University, 430 South Michigan Avenue, Chicago, Illinois 60605, United States

Supporting Information

ABSTRACT: We have prepared and characterized a Ni complex with an N_3S_2 ligand set (**1**) that represents the first isolable synthetic model of the reduced form of the Ni-SOD (SOD = superoxide dismutase) active site featuring all relevant donor functionality in the proper spatial distribution. As revealed by X-ray crystallography, the axial py-N donor of **1** does not bind Ni^{II} in the solid state or in solution like SOD. Oxidation of **1** provides a disulfide-linked dinuclear species, $[\{Ni(N_3S_2)\}_2]$ (**2**), which we have isolated and characterized. Moreover, the **1** → **2** conversion is reversible, much like redox cycling in the enzyme.

Superoxide dismutases (SODs) are crucial metalloenzymes that maintain and regulate superoxide ($O_2^{\bullet-}$) levels in many aerobic organisms, including humans, and are essential for overall health and survival.[1] Ni-SODs,[2−5] however, are true outliers in the SOD family; they have little in common structurally or spectroscopically with other SODs and offer a new perspective on reactive oxygen species (ROS) regulation in biology. In the reduced Ni^{II} state (Ni-SOD_{red}), the Ni ion is contained in an unprecedented environment consisting of one primary amine-N, one anionic carboxamido-N, and two thiolato-S donors to complete a square-planar NiN_2S_2 coordination motif (Chart 1).[3] In the Ni^{III} state (Ni-SOD_{ox}), the geometry changes to square-pyramidal via axial ligation of the His1 imidazole-N (Chart 1).[3] Ni-SOD represents one of the few examples of a metallosulfur-based enzyme that is directly involved in ROS control,[6] because of the deleterious O_2 reactivity associated with Cys-S.[7] Furthermore, although not ubiquitous in biology, the carboxamido-N/thiolato-S motif has been found in only a handful of metalloenzymes that catalyze very different reactions,[8] none of which involve ROS or O_2 activaton. Thus, understanding the fundamental chemistry that occurs at this unusual Ni cofactor could have potential implications in health[9] and in chemical synthesis via Ni-catalyzed O_2 activation.[10]

Designing and constructing small-molecule analogues is one such mechanism to further our understanding of this complex metalloenzyme. However, assembling a true structural and functional model of the Ni-SOD active site is a formidable task because of the inherent difficulties associated with metallosulfur chemistry. To date, models have been dominated by peptide maquettes,[11] small peptides,[12] and discrete low-molecular-weight systems with both approximate[13] and accurate[14] Ni-SOD coordination spheres.

Chart 1. Active Site of Ni-SOD in the Oxidized (Left) and Reduced (Center) States and the Model Used in This Study (Right)

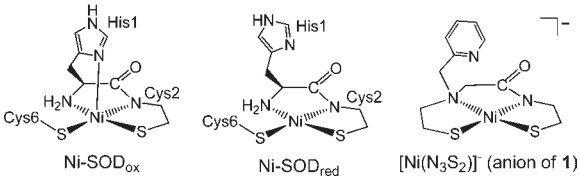

Excluding the functional maquettes, none have reproduced the *exact* N_3S_2 set found at the active site. Indeed, the presence of the axial N-donor is notably absent from all Ni-SOD models.[15] The axial N-His is postulated to play a role in stabilizing Ni^{III}, and mutants lacking this ligand display almost no activity.[3b,4b] Clearly, the study of this interaction in a well-defined model will provide a step toward understanding the mechanism of this enzyme. Herein, we present the synthesis and properties of $K[Ni(N_3S_2)]$ (**1**) as the first Ni-SOD_{red} model containing a *spatially and electronically accurate* N_3S_2 ligand frame.

Red crystals of **1** were obtained over 48 h by recrystallization from 1:1 MeOH/Et_2O at RT. Analogous to Ni-SOD_{red}, the Ni^{II} ion in **1** is housed in a mixed amine/carboxamide/dithiolate square-planar N_2S_2 environment, with the N of the appended py unbound but in close proximity (∼3.2 Å) to Ni (Figure 1 and Table S2 in the Supporting Information, SI). As observed in other Ni-SOD models[14] and in Ni-SOD_{red} from *S. seoulensis*,[3b] the Ni−$N_{carboxamide}$ bond distance is shorter [1.8575(2) Å] than the Ni−N_{amine} bond [1.954(2) Å] because of strong carboxamide σ donation. The noncoordinated py-N is situated 3.210 Å from Ni with its lone pair pointed ∼50° away from the NiN_2S_2 plane. The structural disposition of the py-N of **1** is nearly identical with that of His1-N of Ni-SOD_{red}, which is twisted ∼55−60° from Ni and poised to coordinate via rotation of the His1 Cβ−Cγ bond.[3] Thus, as in Ni-SOD_{red}, Ni^{II} has no affinity for being five-coordinate (5C) in the absence of substrate, and complex **1** serves as a near-identical structural analogue.

The solution properties of **1** are typical of most square-planar $Ni^{II}N_2S_2$ complexes[14,16] and confirm that the solid- and solution-state structures are the same ($S = 0$ by ^{1}H NMR, λ_{max} = 449 and 570 nm in MeOH; see the SI). Cyclic voltammetry (CV)

Received: August 22, 2011
Published: September 02, 2011

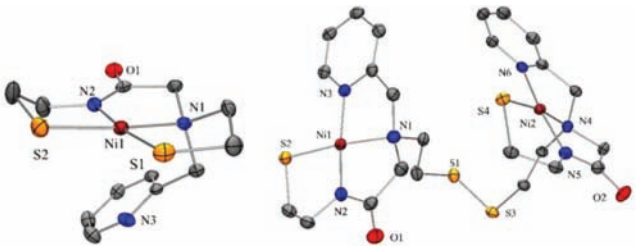

Figure 1. ORTEP diagrams of one of the unique anions of **1** (left) and **2** (right) showing 50% thermal probability ellipsoids for all non-H atoms.

measurements of **1** display an irreversible oxidation (E_{ox}) event in DMF at −0.62 V vs Fc/Fc^+ (−0.45 V in MeOH; see the SI) due to structural rearrangement brought about by the thiyl radical and eventual disulfide formation (vide infra). The electrochemical behavior of **1** is not surprising considering the nearly equal Ni and S (if not more S) contribution in the HOMO of **1** (vide infra), Ni-SOD_{red}, and other models.[4c,14] Other electronically accurate models with only N_2S_2 frames exhibit similar irreversible or quasi-reversible $Ni^{II/III}$ couples,[14] suggesting that introduction of the py-N ligand in the model is insufficient to affect pure Ni-based redox like in SOD. It appears evident from this work that ligand redox in the enzyme is prevented by steric factors arising from its packed quaternary structure, which limits access to the active site and especially the cysteinates.[3] This structural fortification may account for the protection of specific thiolate ligands from S-modification in other metallosulfur enzymes such as superoxide reductase (Cys-S located trans to the substrate binding site with substantial peptide−NH---S hydrogen bonding)[6] and nitrile hydratase (where the axial Cys-S is *not* post-translationally modified to Cys-SO or Cys-SO_2).[8b]

To better understand the nature of the species representative of E_{ox} of **1**, bulk oxidation was performed with ferrocenium (Fc^+). The addition of 1 mol-equiv of $FcPF_6$ to **1** in DMF at −41 °C, followed by slow warming to RT, resulted in a brown-orange solution, where orange solids of the disulfide $[\{Ni(N_3S_2)\}_2]$ (**2**) were isolated. The formation of **2** is a clean process, and no other Ni product was identifiable via ^1H NMR or ESI-MS. Crystallographic analysis of **2** revealed two nearly identical square-planar $Ni^{II}N_3S$ units connected via a symmetric disulfide linkage originating from the thiolato S *trans to the carboxamido-N* of **1** (Figure 1). Occupying the position of the displaced S is the previously unbound py-N to complete the NiN_3S motif. The Ni−N and Ni−S bond lengths are contracted relative to **1** and are consistent with the weaker ligand field as RS^- is replaced by py-N. The most significant difference is found in the Ni−$N_{carboxamide}$ bond, which has contracted 0.020 Å to 1.8371(19) Å (average of the Ni centers). The Ni−S and Ni−N_{amine} bonds correspondingly contract by ∼0.01 Å to 2.1603(6) and 1.9462(19) Å, respectively. The new Ni−N_{py} bond of 1.8945(19) Å is comparable to those of other Ni complexes.[10b,14a,14b] CV measurements of **2** in DMF display E_{red} at −1.84 V (vs Fc/Fc^+), which matches E_{red} found in CVs of **1** *only when scanning from the positive direction* (Figures S6 and S7 in the SI); i.e., the formation of **2** from **1** and vice versa are coupled processes. In support of this observation, no E_{ox} is observed in CVs of **2** when scanning in the oxidative direction and no E_{red} resulted when initiating CVs of **1** in the reductive direction. Furthermore, *the* ***1*** → ***2*** *conversion is reversible* as treatment of **2** with 2 mol-equiv of $[Co(Cp^*)_2]$ resulted in the quantitative regeneration of **1**.

Scheme 1. Proposed Mechanism of the 1→ 2 Interconversion; Hypothesized Intermediates in Red Brackets

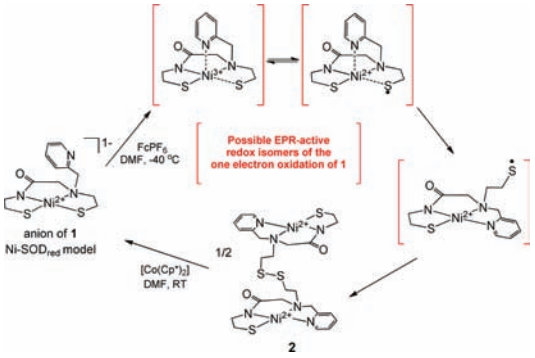

DFT calculations (OLYP/def2-TZVPP) provide further insight into the electronic nature and reactivity of this Ni-SOD model. DFT-optimized structures for **1** are in good agreement with the X-ray structure (Figure S18 in the SI). The carboxamide-N atom is the most negatively charged donor, which is consistent with the observed trans influence, i.e., the slight elongation of the Ni−S1 bond relative to Ni−S2. Moreover, S1 possesses a slightly more negative charge than S2, making it the more probable location for any ligand-based oxidation that might occur. The HOMO of **1**, although primarily based on Ni, contains significant contributions from S (58% Ni and 31% S). DFT predicts that, upon oxidation, a pseudo-trigonal-bipyramidal (τ = 0.51) intermediate is formed, with N1 and S2 becoming axial. In this structure, the unpaired electron has major spin density (64%) on Ni and a minor spin (23%) located on S1, which is symptomatic of a covalent Ni−S bond. Notwithstanding the lack of steric protection offered by the protein in Ni-SOD, the Ni in **1** is suitably tuned by the ligand to support metal-based redox. Upon oxidation, the Ni−N3 separation decreases from 3.81 to 2.17 Å, with a concomitant 0.04 Å contraction of Ni−S1. In support of the formation of **2**, an alternative oxidized (neutral spin doublet) form was also investigated, in which the py-N3 replaces S1 in a monomeric square-planar Ni^{II} species. This complex displays predominant spin density localized on S1 as a free thiyl radical (Figure S24 in the SI). This alternative oxidized structure is likely responsible for the sharp signal observed in the EPR (Figure S1 in the SI) and is a potential precursor to the formation of **2** (Scheme 1, vide infra).

The structural conversion between **1** and **2**, albeit different, does mimic the Ni-SOD_{red} → Ni-SOD_{ox} redox structural change, i.e., coordination of the axial N donor upon oxidation. In line with this comparison, the formation of a paramagnetic intermediate at S or Ni must occur in the **1** → **2** conversion, with most of the spin density likely on S1 of **1** to result in **2**. DFT calculations further confirm this proposal (vide supra). To better understand this conversion, we trapped intermediates formed in situ after the addition of Fc^+ by utilizing EPR. The EPR spectrum revealed an isotropic signal at g = 2.00 that likely originates from an S-based (thiyl) radical (Figure S1 in the SI). Also observed is an anisotropic signal with a large g spread ($\mathbf{g}$ = [2.26, 2.17, ∼2.00]), indicating Ni^{III}. Indeed, these features are similar to those observed in Ni-SOD_{ox} ($\mathbf{g}$ = [2.30, 2.22, 2.01])[3a,4] and the few synthetic square-pyramidal $Ni^{III}N_3S_2$ species.[16] The expected g_z signal from Ni^{III} is not detected in the EPR, but simulation of this data suggests that it is likely coincidental with the S-radical signal (Figure S1 in the SI).

dx.doi.org/10.1021/ic201822f |*Inorg. Chem.* 2011, 50, 9216–9218

In conclusion, we have presented the synthesis and properties of the first structural *and* electronic biomimetic of Ni-SOD$_{red}$ (**1**). We also present the first example of a structurally characterized complex that binds an axial N donor (via a proposed 5C transition state) during oxidation of the Ni-SOD$_{red}$ model **1** to form **2** via a defined and reversible reaction path.[17] While our results suggest that the axial His-1-Im ligand in Ni-SOD is not entirely responsible for Ni-based redox, it still appears crucial for keeping the coordination sphere intact to prevent polymeric RSSR formation. Thus, His1-N binding *in combination with* the protein structure is primarily responsible for $Ni^{II/III}$ cycling in Ni-SOD. Further support for this hypothesis comes from theoretical studies on truncated forms of the enzyme,[4c] which suggest a primarily S-based HOMO in Ni-SOD$_{red}$ along with a long $Ni^{III}N_{im}$ distance (~2.5 Å) for Ni-SOD$_{ox}$.[3] Furthermore, of the few stable Ni^{III} thiolate complexes generated from $Ni^{II}N_2S_2$ precursors,[16] many utilize both additional exogenous N donors and some form of steric protection at the thiolates. In fact, only one Ni^{III} thiolate species has ever been crystallized,[16a] underscoring the difficulty in Ni thiolate[18] chemistry and, in retrospect, Nature's unique design of Ni—biochemical systems.[1] Current efforts are underway to incorporate more robust thiolates into similar Ni-(N_3S_2) constructs for improved stability and function.[19,20]

■ ASSOCIATED CONTENT

Supporting Information. Details of the syntheses, reactivity, spectroscopic, crystallographic (CIF), and computational results. This material is available free of charge via the Internet at http://pubs.acs.org.

■ AUTHOR INFORMATION

Corresponding Author
*E-mail: tharrop@uga.edu.

■ ACKNOWLEDGMENT

T.C.H. and H.F.S. acknowledge the NSF (CAREER CHE-0953102 and CHE-1054286, respectively) for support. We dedicate this paper to the late Prof. Michelle Millar for her tremendous contributions to metal thiolate chemistry.

■ REFERENCES

(1) Valentine, J. S.; Wertz, D. L.; Lyons, T. J.; Liou, L.-L.; Goto, J. J.; Gralla, E. B. *Curr. Opin. Chem. Biol.* **1998**, *2*, 253.

(2) (a) Youn, H.-D.; Kim, E.-J.; Roe, J.-H.; Hah, Y. C.; Kang, S.-O. *Biochem. J.* **1996**, *318*, 889. (b) Youn, H.-D.; Youn, H.; Lee, J.-W.; Yim, Y.-I.; Lee, J. K.; Hah, Y. C.; Kang, S.-O. *Arch. Biochem. Biophys.* **1996**, *334*, 341.

(3) Ni-SOD X-ray structures: (a) Barondeau, D. P.; Kassmann, C. J.; Bruns, C. K.; Tainer, J. A.; Getzoff, E. D. *Biochemistry* **2004**, *43*, 8038. (b) Wuerges, J.; Lee, J.-W.; Yim, Y.-I.; Yim, H.-S.; Kang, S.-O.; Carugo, K. D. *Proc. Natl. Acad. Sci. U.S.A.* **2004**, *101*, 8569.

(4) Ni-SOD spectroscopic and mutagenesis studies: (a) Bryngelson, P. A.; Arobo, S. E.; Pinkham, J. L.; Cabelli, D. E.; Maroney, M. J. *J. Am. Chem. Soc.* **2004**, *126*, 460. (b) Szilagyi, R. K.; Bryngelson, P. A.; Maroney, M. J.; Hedman, B.; Hodgson, K. O.; Solomon, E. I. *J. Am. Chem. Soc.* **2004**, *126*, 3018. (c) Fiedler, A. T.; Bryngelson, P. A.; Maroney, M. J.; Brunold, T. C. *J. Am. Chem. Soc.* **2005**, *127*, 5449. (d) Herbst, R. W.; Guce, A.; Bryngelson, P. A.; Higgins, K. A.; Ryan, K. C.; Cabelli, D. E.; Garman, S. C.; Maroney, M. J. *Biochemistry* **2009**, *48*, 3354. (e) Ryan, K. C.; Johnson, O. E.; Cabelli, D. E.; Brunold, T. C.; Maroney, M. J. *J. Biol. Inorg. Chem.* **2010**, *15*, 795.

(5) Ni-SOD computations: (a) Pelmenschikov, V.; Siegbahn, P. E. M. *J. Am. Chem. Soc.* **2006**, *128*, 7466. (b) Prabhakar, R.; Morokuma, K.; Musaev, D. G. *J. Comput. Chem.* **2006**, *27*, 1438. (c) Mullins, C. S.; Grapperhaus, C. A.; Kozlowski, P. M. *J. Biol. Inorg. Chem.* **2006**, *11*, 617.

(6) Jenney, F. E., Jr.; Verhagen, M. F. J. M.; Cui, X.; Adams, M. W. W. *Science* **1999**, *286*, 306.

(7) Grapperhaus, C. A.; Darensbourg, M. Y. *Acc. Chem. Res.* **1998**, *31*, 451.

(8) (a) Peters, J. W.; Stowell, M. H. B.; Soltis, S. M.; Finnegan, M. G.; Johnson, M. K.; Rees, D. C. *Biochemistry* **1997**, *36*, 1181. (b) Nagashima, S.; Nakasako, M.; Dohmae, N.; Tsujimura, M.; Takio, K.; Odaka, M.; Yohda, M.; Kamiya, N.; Endo, I. *Nat. Struct. Biol.* **1998**, *5*, 347. (c) Miyanaga, A.; Fushinobu, S.; Ito, K.; Wakagi, T. *Biochem. Biophys. Res. Commun.* **2001**, *288*, 1169. (d) Arakawa, T.; Kawano, Y.; Kataoka, S.; Katayama, Y.; Kamiya, N.; Yohda, M.; Odaka, M. *J. Mol. Biol.* **2007**, *366*, 1497. (e) Darnault, C.; Volbeda, A.; Kim, E. J.; Legrand, P.; Vernède, X.; Lindahl, P. A.; Fontecilla-Camps, J. C. *Nat. Struct. Biol.* **2003**, *10*, 271.

(9) Riley, D. P. *Chem. Rev.* **1999**, *99*, 2573 and references cited therein.

(10) (a) Kieber-Emmons, M. T.; Riordan, C. G. *Acc. Chem. Res.* **2007**, *40*, 618. (b) Manuel, T. D.; Rohde, J.-U. *J. Am. Chem. Soc.* **2009**, *131*, 15582.

(11) (a) Neupane, K. P.; Shearer, J. *Inorg. Chem.* **2006**, *45*, 10552. (b) Neupane, K. P.; Gearty, K.; Francis, A.; Shearer, J. *J. Am. Chem. Soc.* **2007**, *129*, 14605. (c) Shearer, J.; Neupane, K. P.; Callan, P. E. *Inorg. Chem.* **2009**, *48*, 10560. (d) Tietze, D.; Breitzke, H.; Imhof, D.; Kothe, E.; Weston, J.; Buntkowsky, G. *Chem.—Eur. J.* **2009**, *15*, 517.

(12) Krause, M. E.; Glass, A. M.; Jackson, T. A.; Laurence, J. S. *Inorg. Chem.* **2011**, *50*, 2479.

(13) (a) Ma, H.; Chattopadhyay, S.; Petersen, J. L.; Jensen, M. P. *Inorg. Chem.* **2008**, *47*, 7966. (b) Ma, H.; Wang, G.; Yee, G. T.; Petersen, J. L.; Jensen, M. P. *Inorg. Chim. Acta* **2009**, *362*, 4563. (c) Jenkins, R. M.; Singleton, M. L.; Almaraz, E.; Reibenspies, J. H.; Darensbourg, M. Y. *Inorg. Chem.* **2009**, *48*, 7280. (d) Mullins, C. S.; Grapperhaus, C. A.; Frye, B. C.; Wood, L. H.; Hay, A. J.; Buchanan, R. M.; Mashuta, M. S. *Inorg. Chem.* **2009**, *48*, 9974. (e) Gennari, M.; Orio, M.; Pécaut, J.; Neese, F.; Collomb, M.-N.; Duboc, C. *Inorg. Chem.* **2010**, *49*, 6399. (f) Ma, H.; Petersen, J. L.; Young, V. G., Jr.; Yee, G. T.; Jensen, M. P. *J. Am. Chem. Soc.* **2011**, *133*, 5644.

(14) (a) Shearer, J.; Zhao, N. *Inorg. Chem.* **2006**, *45*, 9637. (b) Gale, E. M.; Patra, A. K.; Harrop, T. C. *Inorg. Chem.* **2009**, *48*, 5620. (c) Gale, E. M.; Narendrapurapu, B. S.; Simmonett, A. C.; Schaefer, H. F., III; Harrop, T. C. *Inorg. Chem.* **2010**, *49*, 7080. (d) Mathrubootham, V.; Thomas, J.; Staples, R.; McCraken, J.; Shearer, J.; Hegg, E. L. *Inorg. Chem.* **2010**, *49*, 5393.

(15) No exact model exists; however, complexes by Jensen[13a,13b,13f] have approximated the N_3S_2 core.

(16) (a) Krüger, H.-J.; Peng, G.; Holm, R. H. *Inorg. Chem.* **1991**, *30*, 734. (b) Hanss, J.; Krüger, H.-J. *Angew. Chem., Int. Ed.* **1998**, *37*, 360. (c) Fiedler, A. T.; Brunold, T. C. *Inorg. Chem.* **2007**, *46*, 8511. (d) Gennari, M.; Orio, M.; Pécaut, J.; Bothe, E.; Neese, F.; Collomb, M.-N.; Duboc, C. *Inorg. Chem.* **2011**, *50*, 3707. (e) Stenson, P. A.; Board, A.; Marin-Becerra, A.; Blake, A. J.; Davies, E. S.; Wilson, C.; McMaster, J.; Schröder, M. *Chem.—Eur. J.* **2008**, *14*, 2564.

(17) Langford, C. H.; Gray, H. B. *Ligand Substitution Processes*; W. A. Benjamin: New York, 1966.

(18) Albela, B.; Bothe, E.; Brosch, O.; Mochizuki, K.; Weyhermüller, T.; Wieghardt, K. *Inorg. Chem.* **1999**, *38*, 5131.

(19) Fox, S.; Wang, Y.; Silver, A.; Millar, M. *J. Am. Chem. Soc.* **1990**, *112*, 3218.

(20) Like Ni-SOD complex **1** has no affinity for excess N_3^- (DMF). No reaction of **1** with excess KO_2 was observed in DMF, while performing the reaction in pH 7.5 PIPES afforded S-oxygenates presumably due to the spontaneous disproportionation of superoxide in water and formation of H_2O_2 (see the SI).